Erik Jonsson School of Engineering and Computer Science

Decoupling the Influence of Surface Structure and Intrinsic Wettability on Boiling Heat Transfer

UT Dallas Author(s):

Xianming (Simon)Dai

Citation:

Dai, X., P. Wang, F. Yang, X. Li, et al. 2018. "Decoupling the influence of surface structure and intrinsic wettability on boiling heat transfer." Applied Physics Letters 112(25), doi:10.1063/1.5030420

Decoupling the influence of surface structure and intrinsic wettability on boiling heat transfer

Xianming Dai,[1,2,a)] Pengtao Wang,[1,a)] Fanghao Yang,[1] Xiaochuan Li,[3] and Chen Li[1,b)]
[1]*Department of Mechanical Engineering, University of South Carolina, Columbia, South Carolina 29208, USA*
[2]*Department of Mechanical Engineering, University of Texas at Dallas, Richardson, Texas 75080, USA*
[3]*School of Hydraulic, Energy and Power Engineering, Yangzhou University, Yangzhou, Jiangsu 225127, China*

(Received 21 March 2018; accepted 7 June 2018; published online 20 June 2018; corrected 29 June 2018)

Surface structure and intrinsic wettability are both important for boiling heat transfer. While superhydrophilic micro, nano, and hierarchical surfaces are widely used for boiling enhancement, in which the surface structure and intrinsic wettability usually couple together. This study aims to decouple their influences on boiling heat transfer. Copper meshes are utilized as the microporous structures, and conformal superhydrophilic films of TiO_2 are deposited by atomic layer deposition (ALD). Although ALD coatings for boiling have been done on flat surfaces, this study separates the influence of surface structure from that of intrinsic wettability on a three-dimensional microporous surface. By comparing two and four layer meshes, we show that the surface structure has no obvious influence on the critical heat flux (CHF), but can significantly enhance the heat transfer coefficient (HTC). The intrinsic superhydrophilicity dramatically increases the CHF due to the fast rewetting of dryout regions. Our conclusion is that fast rewetting is critical to increase the CHF, while large surface areas are vital to enhance the HTC. *Published by AIP Publishing.*
https://doi.org/10.1063/1.5030420

Boiling heat transfer exhibits promise for improving thermal management by taking the advantage of latent heat.[1] Its performance is evaluated by the heat transfer coefficient (HTC) and the critical heat flux (CHF). HTC is expressed as a ratio of the heat flux, q'', and the wall superheat, $\Delta T_{super} = T_w - T_{sat}$. Here, $q'' = 1/(6\pi\rho_g h_{fg} N_A D_b^3 f_b)$, where ρ_g is the vapor density, h_{fg} is the specific enthalpy, N_A is the number of active nucleation sites, D_b is the bubble departure diameter, and f_b is the bubble departure frequency.[2] These equations indicate that the HTC, at a given wall superheat, can be enhanced by increasing the active nucleation site density and/or manipulating the bubble dynamics. Experimental studies reveal that the active nucleation site density can be significantly increased using multi-scale structures, for example, microstructures,[3,4] nanostructures,[5,6] and hierarchical structures.[7,8] The bubble dynamics on a heated wall depend on the surface structures and wettability.[9] As described by the Fritz model,[10] a hydrophilic smooth surface yields vapor bubbles with smaller departure diameters and higher departure frequencies.[11] CHF indicates a boiling crisis,[12] where the boiling surface is insulated by a coalescence of densely packed bubbles or a vapor film, which sharply increases the wall temperature. Most hydrophilic surfaces offer a smaller HTC and a higher CHF than hydrophobic surfaces.[13] Compared with a hydrophilic surface, a superhydrophilic surface slightly changes the HTC, but significantly improves the CHF.[14]

The major enhancement mechanisms of pool boiling can be summarized as increased nucleation site density resulting from the augmented surface areas, and enhanced bubble growth rate enabled by the intrinsic wettability. These two factors are usually coupled together and are widely known as the Wenzel's effects.[15,16] Few experiments separated the effects of intrinsic wettability from surface morphology using smooth surfaces, such as flat surfaces[17] and Pt wires.[14] The intrinsic wettability can be altered by coating a thin hydrophobic or hydrophilic film, such as alkanethiol[17] or Teflon[18] for hydrophobicity, and SiO_2[18] or Al_2O_3[14] for hydrophilicity. It is challenging to separate these two factors on three-dimensional (3-D) microporous boiling surfaces.

This study focuses on decoupling the influence of 3-D surface structure and intrinsic wettability on boiling heat transfer. The surface structures are provided by copper woven meshes (wire diameter 56 μm, mesh number 145 inch^{-1}, Belleville Wire Cloth Co., NJ), which are sintered on a copper block in a nearly perfect thermal contact condition.[19] 2-layer and 4-layer copper meshes are fabricated 0.21 mm thick and 0.37 mm thick with a porosity of 0.72 and 0.69, respectively. The intrinsic wettability of copper mesh is modified by coating a thin film of TiO_2 in an atomic layer deposition (ALD) reactor (see the supplementary material for the detailed ALD process). ALD is the known best method for coating a conformal film on high aspect ratio micro/nanostructures.[20] High conformality of ALD TiO_2 coating was achieved, which was visualized with a FIB-SEM on the cross section of ALD TiO_2 coated nanowires (shown in the supplementary material). It also showed that a 20 nm of this ALD TiO_2 coating produced a stable wettability, and more information on this coating can be found in Refs. 21 and 22.

The ALD TiO_2 coating retains the original surface morphology of individual copper mesh wire [Figs. 1(a) and 1(b)]. The root means square roughness (RMS) slightly

[a)]X. Dai and P. Wang contributed equally to this work.
[b)]Author to whom correspondence should be addressed: li01@cec.sc.edu

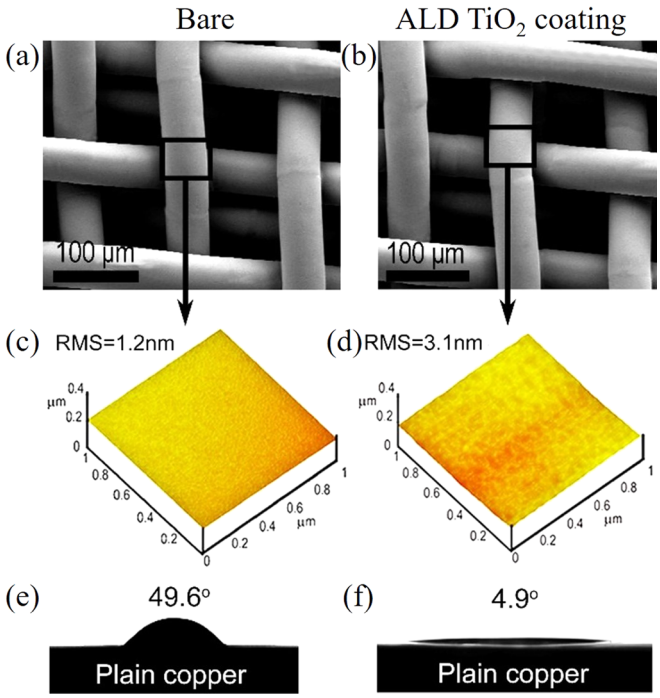

FIG. 1. Characterization of the bare and ALD TiO_2 coated copper meshes. SEM image of (a) bare copper meshes, (b) copper meshes with ALD TiO_2 coating, (c) AFM image of the surface topography on (c) a single bare copper wire, and (d) copper wire with ALD TiO_2 coating. Contact angle of 5 μl water droplet on (e) bare plain copper surface, and (f) plain copper surface with ALD TiO_2 coating.

increases from 1.2 nm of the bare copper wire to 3.1 nm after being coated with ALD TiO_2 [Figs. 1(c) and 1(d)]. Compared with surfaces modified with the other techniques,[23] the ALD TiO_2 coating shows great conformity and negligible increment of roughness; hence, the surface area augmentation seems insignificant. However, the ALD TiO_2 coating significantly improves the wettability. The inherent contact angle on a bare plain copper surface reduces from 49.6° to 4.9° after the application of an ALD TiO_2 coating [Figs. 1(e) and 1(f)]. It indicates that the intrinsic water affinity of TiO_2 can significantly improve the hydrophilicity of an individual copper mesh wire, which is different from the apparent superhydrophilicity resulting from the surface roughness.[6] The apparent contact angle on the ALD TiO_2 coated 2-layer meshes is nearly 0°, as predicted by the Wenzel's law.[16]

The pool boiling experiments are conducted under steady-state conditions at atmospheric pressure using deionized water (see the supplementary material for the experimental system and data reduction). The surface structures, fabricated by sintering 2-layer and 4-layer copper meshes, are annotated as "2L" and "4L"; the intrinsic wettability, modified without/with a coating of ALD TiO_2, are annotated as "Bare" and "TiO_2." For each surface structure and wettability, two samples are fabricated at the same time, annotated as "S1" and "S2." A total of 8 samples is experimentally tested and reported in Fig. 2. Plain copper surface is tested to calibrate the system,[24] and its results serve as the baseline for comparison (annotated as "Plain, Bare" in Fig. 2).

Boiling heat transfer on 2-layer-mesh and 4-layer-mesh without/with an ALD TiO_2 coating is experimentally evaluated. Experimental results presented as heat flux vs.

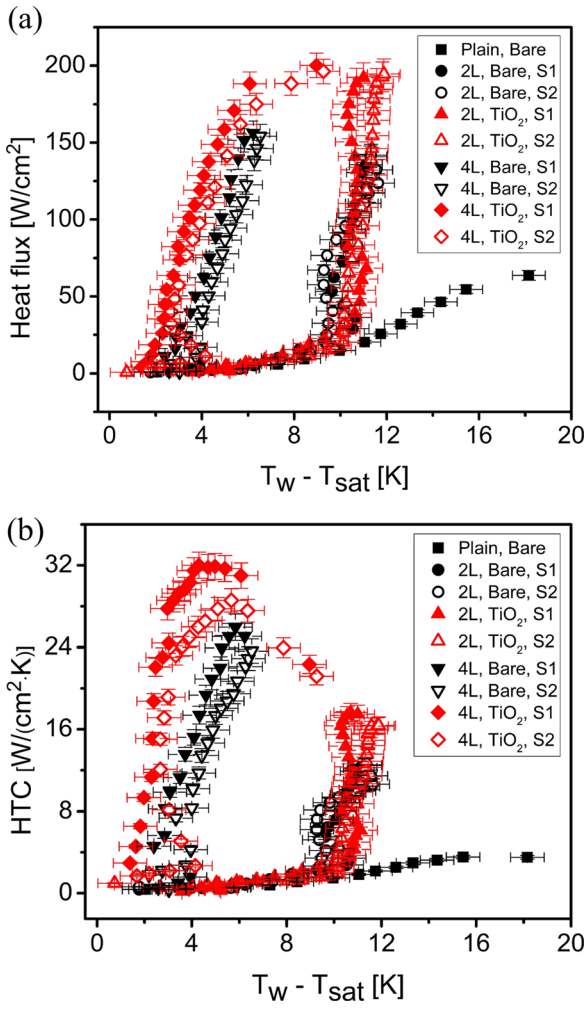

FIG. 2. Effects of surface structure and intrinsic wettability on the boiling heat transfer performance. (a) Heat flux vs. wall superheat and (b) HTC vs. wall superheat.

superheat and HTC vs. superheat are shown in Fig. 2. The curves of HTC vs. heat flux are provided as the supplementary material. A relatively low CHF is achieved on a well-polished plain bare surface, which is consistent with the CHF on smooth oxidized silicon surfaces.[3] Slight variations in the onset of nucleation for coated samples are observed, which is likely due to surface wettability rather than surface defects. This claim is supported by the fact that the HTC on the ALD TiO_2 coated 2-layer meshes is not greatly increased (or slightly changed).[7] Both the HTC and the CHF are significantly improved by the 2-layer-mesh, compared with these on the plain surface. The reason is that the rewetting on plain surfaces is not strong due to the lack of capillarity.[25] On the 2-layer-mesh without/with a TiO_2 coating and the bare 4-layer-mesh, heat flux increases linearly with the wall superheat, and the HTC on the 2-layer-mesh is much lower than that on the 4-layer-mesh. Previous studies have proved that both nucleate boiling and thin film evaporation occurred inside the microstructures.[4,6] The 2-layer-mesh, as a thin capillary structure, cannot well control the water distribution within its structure.[24] The flooding condition on the heated surface results in losing activity of nucleation sites and inhibiting the formation of thin film evaporation. The 4-layer-mesh, with two more layers of meshes, substantially improves the

HTC, because of increased nucleation site density and enlarged surface area for thin film evaporation. For example, at a heat flux of 100 W/cm^2, the HTC is 9.6 ± 0.5 W/(cm^2 K) and 20.9 ± 1.0 W/(cm^2 K) on the 2-layer-mesh and the 4-layer-mesh without an ALD TiO_2 coating, respectively. This doubled HTC on the 4-layer-mesh over the 2-layer mesh is consistent with the area increase ratio.

The effects of the ALD TiO_2 coating on HTC are closely related to the thickness of copper meshes. On the 2-layer-mesh, there is no obvious additional HTC enhancement after the ALD TiO_2 coating. The HTC slightly reduces in the heat flux range of 50 W/cm^2 and 100 W/cm^2 [Fig. 2(b)], indicating that the superhydrophilic coating adopted in this study cannot effectively enhance or even deteriorate the HTC. This fact is that the ALD TiO_2 coating on a given structure cannot introduce more nucleate sites; on the contrary, the resulting superwetting feature tends to deactivate cavities because of flooding. On the 4-layer-mesh with an ALD TiO_2 coating, the HTC is slightly improved at low heat fluxes, but significantly enhanced when heat flux exceeds 50.0 W/cm^2. At a low heat flux, nucleate boiling dominates the boiling process, which cannot be enhanced using superhydrophilic coatings. At higher heat fluxes, more vapor bubbles form on the porous structures and thin film evaporation dominates. As a result, the HTC, on the 4-layer-mesh with an ALD TiO_2 coating, increases from 20.9 ± 1.0 W/(cm^2 K) to 29.3 ± 1.2 W/(cm^2 K) at a heat flux of 100 W/cm^2. After heat fluxes exceed 161.8 W/cm^2, the HTC remains constant or slightly decreases until reaching the CHF.

On the 4-layer-mesh with ALD TiO_2 coating, there is an obvious change in the slope of the boiling curves. A relatively stable HTC at high wall superheat has been maintained in a wide range of heat fluxes (161.8–196.2 W/cm^2) prior to the CHF. It indicates that there is a heat transfer mode between nucleate boiling and film boiling. This mode occurs on the 4-layer-mesh with ALD TiO_2 coating, and it is called "II nucleate boiling"[26] with a high vapor fraction (i.e., partial dry out). These significant differences in boiling curves have been extensively observed on the porous coatings with various thicknesses, where the formation of a vapor film was hypothesized.[27] It has been shown that this vapor film has a critical thickness about 2–5 times of the particle size,[28] corresponding to 0.96–2.39 mm of the copper meshes used in this research. Our previous experiments[4] demonstrated that the similar condition was achieved on the identical copper meshes, which consisted of 16–32 layers (the thickness is 1.38–2.30 mm). It reveals that such a critical thickness during boiling on the porous structures can be significantly reduced using a superhydrophilic coating. The ALD TiO_2 coating yields a lower vapor pressure (due to a smaller superheat) and a higher surface tension at the liquid-vapor-solid lines. The coating, therefore, tends to pin the vapor-liquid interface on the copper wires.[29]

During the boiling process, the heat transfer performance depends mainly on the wetting condition on the heated surface, which can be identified from the liquid distribution beneath a growth bubble: macrolayer, microlayer, and dryout region[30] [Fig. 3(a)]. In addition, thin film evaporation on the microlayer plays a dominant role in the HTC.[31] The flooded condition in the 2-layer-mesh makes it difficult to form microlayers and dryout regions on the heating surface.

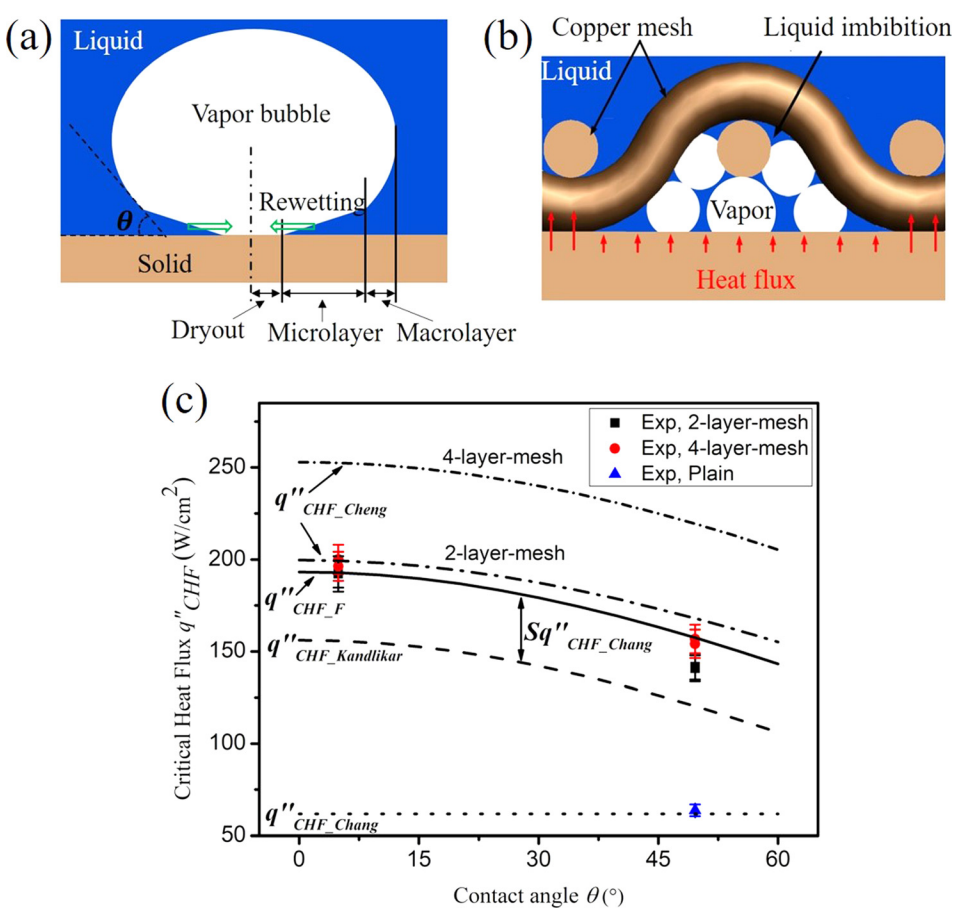

FIG. 3. Boiling heat transfer mechanism on copper meshes. (a) Rewetting the microlayer enhanced by ALD TiO_2 coating, (b) liquid imbibition by the surface structures, and (c) empirical CHF models.

As thickness increases on the 4-layer-mesh, the macrolayer can be well maintained because of competition between liquid flow resistance and liquid imbibition driven by the capillary pressure [Fig. 3(b)]. When the input heat flux increases, more vapor bubbles are generated, providing more microlayer regions for thin film evaporation. Therefore, the HTC is continuously enhanced with increased heat flux on the 4-layer-mesh. On a superhydrophilic surface, the profile of microlayer is stretched with extended length and reduced thickness.[32] The region of microlayer is therefore further enlarged on the ALD TiO_2 coated 4-layer-mesh, resulting in additional enhancements of the HTC. When heat flux increases further, part of wick structure dries out, which greatly reduces the thin film evaporation area and lowering the HTC.

CHF is triggered when liquid imbibition driven by the capillary pressure fails to compensate the evaporated fluid,[29] resulting in total dry out. On the 2-layer-mesh without/with TiO_2 coating and bare 4-layer-mesh, nucleate boiling changes to film boiling in a short time at the CHF, where a peak HTC is achieved. On the ALD TiO_2 coated 4-layer-mesh, after the heat flux exceeds 161.8 W/cm^2, HTC remains constant or slightly decreases until reaching the CHF, which implies an active capillarity still occurs even when the wick structure locally dries out.[24] As shown in Fig. 2, the intrinsic wettability, rather than the surface structure, obviously affects the CHF. Typically, the CHF is 141.8 ± 7.1 W/cm^2 and 154.2 ± 8.0 W/cm^2 on the 2-layer-mesh and the 4-layer-mesh with bare surfaces, and 194.5 ± 9.7 W/cm^2 and 196.8 ± 7.8 W/cm^2 for those with ALD TiO_2 coatings, respectively. It indicates that capillary pressure generated from the surface structure has no obvious effects on the CHF on the 2-layer-mesh and the 4-layer-mesh. The capillary pressure (P_{cap}) is given as

$$p_{Cap} = \frac{2\sigma\cos(\theta)}{r_{eff}}, \tag{1}$$

where θ is the contact angle, and r_{eff} is the effective pore radius. The capillary pressure generated inside the copper meshes is about 1.0 kPa, which is much smaller than the hydrostatic pressure ($P_{static} \sim 102.7$ kPa). Equation (1) indicates that the capillary pressure, at a low heat flux, remains constant on the 2-layer and 4-layer meshes due to the fixed pore size. At a high heat flux, the liquid meniscus recedes into the corners between the copper wires, resulting in a significant increase in the capillary pressure. However, this situation may not occur on the 2-layer-mesh, where the heated surfaces are flooded with abundant water supply. Our previous research showed that this flooding condition typically occurred in wick structures with higher porosity, larger pore size, and/or smaller thickness.[24,33] It may occur on the bare 4-layer-mesh, but its effects on the CHF may be suppressed by local dry out on the heated surface at high heat fluxes, because the dry out leads to a loss of capillary pressure. The ALD TiO_2 coating significantly enhances the CHF, representing an increment of 37.2% and 27.6% on the 2-layer-mesh and the 4-layer-mesh, respectively. These enhancements occur because the superhydrophilic ALD TiO_2 coating enables fast superwetting to the dryout areas on heated surfaces,[34] as shown in Fig. 3(a). Moreover, the CHF on the ALD TiO_2 coated 2-layer-mesh decreases slightly from 194.5 W/cm^2 to 183.3 W/cm^2 when the surface roughness increases from 3.1 nm to 13.2 nm (in which a TiO_2 coating was prepared with the same chemicals but was produced by a different ALD process).[35] This further confirms that the postponed CHF primarily results from the improved interfacial wettability, rather than augment nanoscale surface roughness.

The mechanism of CHF can be interpreted by a hydrodynamics instability model[36] or a viscous capillary model.[37] Considering the effects of the critical hydrodynamic instability wavelength and the capillary wicking force, the CHF on copper meshes can be empirically predicted by Cheng's model,[38] given as

$$q''_{CHF\_Cheng} = K_{Cheng} q''_{CHF} = K_{Cheng} h_{fg} \rho_v^{1/2} [\sigma g(\rho_l - \rho_v)]^{1/4}, \tag{2}$$

where q''_{CHF} is the general form of CHF. K_{Cheng} is the dimensionless CHF for Cheng's model, and it is

$$K_{Cheng} = \left(\frac{1+\cos\theta}{16}\right)\left[\frac{2}{\pi}\left(1-\sqrt{\phi_s}\right)^{-1/2}\frac{\psi+\cos\theta}{1+\cos\theta} + \frac{\pi}{4}\left(1-\sqrt{\phi_s}\right)^{1/2}(1+\cos\theta)\right]^{1/2}, \tag{3}$$

where ϕ_s and ψ are the solid fraction and the roughness factor of sintered copper meshes, respectively. On the 2-layer-mesh, $\phi_s = 0.28$ and $\psi = 4.46$; while on the 4-layer mesh, $\phi_s = 0.31$ and $\psi = 8.91$. The roughness factor in Eq. (3) is a physical parameter, which is calculated from the surface area of single layer mesh and the number of layers. There is a consistency between experimental and theoretical CHF on the 2-layer-mesh, especially for that with an ALD TiO_2 coating. Cheng's model predicts a higher value of the CHF on the 4-layer-mesh than that determined experimentally, as shown in Fig. 3(c). A previous study indicated that the exposed surface of sintered copper meshes remained constant, regardless of the layers of copper meshes.[24] It is more reasonable to replace the physical roughness factor (ψ) with the effective one (ψ_{eff}) in Cheng's model, which is defined from the actual wetted area. ψ_{eff}, derived from Cheng's model by a mathematical fitting, is 2.5 and 3.4 on the 2-layer-mesh and the 4-layer-mesh with bare surfaces, and ψ_{eff} increases to 4.0 and 4.3, after ALD TiO_2 coatings are applied, respectively. This further proves that the ALD TiO_2 coating can enlarge the actual wetting area as a result of rewetting the dryout regions. Therefore, CHF can be postponed by the superhydrophilic ALD TiO_2 coating. Extended analysis with other empirical models of CHF presented in Fig. 3(c), such as Kandlikar's model[39] and Chang's model,[40] are discussed in the supplementary material.

In summary, we experimentally and theoretically show that the decoupled effects of surface structure and intrinsic wettability of copper meshes on boiling heat transfer. For the 2-layer-mesh and the 4-layer-mesh used in this research, the surface structure has no obvious effects on the CHF, but it can significantly enhance the HTC. The superhydrophilic

ALD TiO_2 coating dramatically increases the CHF, but it cannot effectively enhance the HTC on the thin wick structure in a flooding condition. We conclude that large exposed surface areas are vital to enhance the HTC, and fast rewetting is critical to increase the CHF.

See supplementary material for (a) the detail of atomic layer deposition of TiO_2, (b) experimental setup, (c) data reduction, (d) experimental data for the effects of surface structure and intrinsic wettability on boiling performance, and (e) analysis with empirical models for the CHF.

This work is supported by the Electric Power Research Institute (EPRI 1-108059-01-05) and partially by the startup funds of the University of South Carolina (USC) to Dr. Chen Li. The authors gratefully acknowledge the George Research Group (P.I.: Dr. Steven George) and the NEXT group (P.I.: Dr. Ronggui Yang) at the University of Colorado Boulder in preparation of ALD TiO_2 coatings. The authors also thank Dr. Miao Yu and Mr. Lei Wang from the Department of Chemical Engineering at USC in the help of characterizing ALD TiO_2 coatings. The authors appreciate Dr. Alam Tamanna at USC for her professional proofreading.

[1]I. Mudawar, J. Therm. Sci. Eng. Appl. **5**(2), 021012 (2013).
[2]I. C. Bang, J. Buongiorno, L.-W. Hu, and H. Wang, J. Power Energy Syst. **2**(1), 340 (2008).
[3]K.-H. Chu, R. Enright, and E. N. Wang, Appl. Phys. Lett. **100**(24), 241603 (2012).
[4]C. Li and G. P. Peterson, J. Heat Transfer **129**(11), 1465 (2007).
[5]J. Kim, S. Jun, J. Lee, J. Godinez, and S. M. You, J. Heat Transfer **139**(10), 101501 (2017).
[6]C. Li, Z. Wang, P.-I. Wang, Y. Peles, N. Koratkar, and G. P. Peterson, Small **4**(8), 1084 (2008).
[7]K.-H. Chu, Y. S. Joung, R. Enright, C. R. Buie, and E. N. Wang, Appl. Phys. Lett. **102**(15), 151602 (2013).
[8]R. Wen, Q. Li, W. Wang, B. Latour, C. H. Li, C. Li, Y.-C. Lee, and R. Yang, Nano Energy **38**, 59 (2017); H. W. Moon, Y. J. Yoon, J. H. Park, B.-S. Myung, and D. E. Kim, Exp. Therm. Fluid Sci. **74**, 19 (2016).
[9]A. Sur, Y. Lu, C. Pascente, P. Ruchhoeft, and D. Liu, Int. J. Heat Mass Transfer **120**, 202 (2018); A. Shahriari, M. Hermes, and V. Bahadur, Appl. Phys. Lett. **108**(9), 091607 (2016).
[10]W. Fritz, Phys. Z. **36**, 6 (1935).
[11]Y. Nam, E. Aktinol, V. K. Dhir, and Y. Sungtaek Ju, Int. J. Heat Mass Transfer **54**(7–8), 1572 (2011).
[12]P. Lloveras, F. Salvat-Pujol, L. Truskinovsky, and E. Vives, Phys. Rev. Lett. **108**(21), 215701 (2012).
[13]A. R. Betz, J. Jenkins, C. J. Kim, and D. Attinger, Int. J. Heat Mass Transfer **57**(2), 733 (2013); X. Dai, X. Huang, F. Yang, X. Li, J. Sightler, Y. Yang, and C. Li, Appl. Phys. Lett. **102**(16), 161605 (2013).
[14]B. Feng, K. Weaver, and G. P. Peterson, Appl. Phys. Lett. **100**(5), 053120 (2012).
[15]X. Dai, B. B. Stogin, S. Yang, and T.-S. Wong, ACS Nano **9**(9), 9260 (2015).
[16]P. Wang, J. Su, M. Shen, M. Ruths, and H. Sun, Langmuir **33**(2), 638 (2017).
[17]B. Bourdon, R. Rioboo, M. Marengo, E. Gosselin, and J. De Coninck, Langmuir **28**(2), 1618 (2012).
[18]H. J. Jo, S. H. Kim, H. Kim, J. Kim, and M. H. Kim, Nanoscale Res. Lett. **7**(1), 242 (2012).
[19]C. Li and G. P. Peterson, Int. J. Heat Mass Transfer **49**(21-22), 4095 (2006).
[20]H. Kim, H.-B.-R. Lee, and W. J. Maeng, Thin Solid Films **517**(8), 2563 (2009).
[21]A. I. Abdulagatov, Y. Yan, J. R. Cooper, Y. Zhang, Z. M. Gibbs, A. S. Cavanagh, R. G. Yang, Y. C. Lee, and S. M. George, ACS Appl. Mater. Interfaces **3**(12), 4593 (2011).
[22]W. Wang, M. Tian, A. Abdulagatov, S. M. George, Y.-C. Lee, and R. Yang, Nano Lett. **12**(2), 655 (2012).
[23]P. Wang, R. Dawas, M. Alwazzan, W. Chang, J. Khan, and C. Li, Int. J. Heat Mass Transfer **111**, 817 (2017); J. Su, M. Charmchi, and H. Sun, Sci. Rep. **6**, 35132 (2016).
[24]C. Li, G. P. Peterson, and Y. Wang, J. Heat Transfer **128**(12), 1312 (2006).
[25]N. S. Dhillon, J. Buongiorno, and K. K. Varanasi, Nat. Commun. **6**, 8247 (2015).
[26]S. P. Malyshenko, Therm. Eng. **38**(2), 81 (1991).
[27]M. Ha and S. Graham, Appl. Phys. Lett. **111**(9), 091601 (2017).
[28]S. Sarangi, J. A. Weibel, and S. V. Garimella, Int. J. Heat Mass Transfer **81**, 103 (2015).
[29]S. G. Liter and M. Kaviany, Int. J. Heat Mass Transfer **44**(22), 4287 (2001).
[30]D. I. Yu, H. J. Kwak, H. Noh, H. S. Park, K. Fezzaa, and M. H. Kim, Sci. Adv. **4**(2), e1701571 (2018); C. Gerardi, J. Buongiorno, L.-W. Hu, and T. McKrell, Int. J. Heat Mass Transfer **53**(19–20), 4185 (2010).
[31]A. Zou, D. P. Singh, and S. C. Maroo, Langmuir **32**(42), 10808 (2016).
[32]A. J. Jiao, H. B. Ma, and J. K. Critser, Int. J. Heat Mass Transfer **50**(15), 2905 (2007).
[33]C. Li and G. P. Peterson, J. Heat Transfer **128**(12), 1320 (2006); J. Thermophys. Heat Transfer **24**(3), 449 (2010).
[34]K. Lee, Q. H. Kim, S. An, J. H. An, J. Kim, B. Kim, and W. Jhe, Proc. Natl. Acad. Sci. **111**(16), 5784 (2014); X. Dai, M. Famouri, A. I. Abdulagatov, R. Yang, Y.-C. Lee, S. M. George, and C. Li, Appl. Phys. Lett. **103**(15), 151602 (2013); H. S. Ahn, H. J. Jo, S. H. Kang, and M. H. Kim, Appl. Phys. Lett. **98**, 071908 (2011).
[35]X. Dai, Ph.D dissertation, University of South Carolina, 2013.
[36]Y. V. Polezhaev and S. A. Kovalev, Therm. Eng. **37**(12), 617 (1990).
[37]K. S. Udell, Int. J. Heat Mass Transfer **28**(2), 485 (1985).
[38]X. Quan, L. Dong, and P. Cheng, Int. J. Heat Mass Transfer **76**, 452 (2014).
[39]S. G. Kandlikar, J. Heat Transfer. **123**, 1071–1079 (2001).
[40]Y. P. Chang, USAEC Report No. TID-14004, Washington, DC, 1961.